## Response to Reviewer 1 of

# Examination of Analytical Shear Stress Predictions for Coastal Dune Evolution

Orie Cecil, Nicholas Cohn, Matthew Farthing, Sourav Dutta, Andrew Trautz
*Earth Surface Dynamics,* egusphere-2024-855

---

**RC:** ***Reviewers' Comment***, AR: Authors' Response, *Manuscript Revisions*

---

**RC 1: Section 3.2.1. – what were the discretisation schemes used in the CFD?**

AR: Second order accurate discretization schemes were used throughout. Specifically, the least squares method is used for determining the cell-centered gradient values with a cell based cubic limiter for the velocity and turbulence quantities. A linear upwind scheme was used for all convective terms, and Laplacian terms employed a linear corrected scheme.

*These details have been added to section 3.2.1 (diff lines 228–231).*

---

**RC 2: Section 3.2.1. – What are the computational boundary dimensions (Length and Height). Please make clear whether in this section that all calculations are 2D.**

AR: The domain height is set to be 200 m over the dune crest; therefore, the height ranges from 202.5 m for $H/L = 0.1$ to 212.5 m for $H/L = 0.5$. The total length of the domain is 425 m with the characteristic length (i.e. the half-length at half-height) of the dunes fixed at 25 m. All CFD simulations were two-dimensional.

*These details have been included in section 3.2.2 (diff lines 244–247).*

---

**RC 3: Section 3.2.1. - Where were the 'dunes' placed in the context of the upwind and downwind boundaries?**

AR: All 'dunes' have their crest at $x = 30$ m while the domain is symmetric about $x = 0$ m. With an overall domain length of 425 m, this places the upstream boundary 242.5 m upwind of the crest and the downstream boundary 182.5 m from the crest.

*These details have been included in section 3.2.2 (diff lines 244–247).*

---

**RC 4: Section 3.2.1 – What $z_0$ value was used in equations 7 to 11? How does this compare to the smallest cell size? ($z_0$ must be below 50% of the bottom cell height as wall function cannot extend above this. See Figure 3 in https://doi.org/10.1016/j.atmosenv.2006.08.019)**

AR: For this study, $z_0$ was held constant at 1e−3 m throughout as specified in section 3.1. The smallest size of the first cell was 5.138e−3 m for the quartic profile with $H/L = 0.5$. However, the wall function implementations

in OpenFOAM that were used (i.e., `atmNutkWallFunction` and `atmEpsilonWallFunction`) are based directly on the aerodynamic roughness length without needing to use an equivalent sand grain roughness height as required for the Fluent and CFX rough wall function implementations. This alleviates the burdensome requirement on the first cell height as discussed in section 7.2 of the reference cited as well as in section 2.2 of Parente et al. 2011 (https://doi.org/10.1016/j.jweia.2010.12.017).

*The minimum cell height for all cases was added in section 3.2.1 (diff lines 248–250).*

---

**RC 5: Line 226 – What is meant by a uniform base discretization?**

AR: SnappyHexMesh requires a simple base discretization which is modified by refinement around object edges (the dune profile in this case), snapping points to object edges, and finally prism inflation. The base discretization for these cases is simply a uniform grid consisting of 1 m $\times$ 1 m cells over the entire domain.

*Slight changes were made in section 3.2.2 to help clarify the meshing procedure (diff lines 247–249).*

---

**RC 6: Line 228 – Please quantify what a 'sufficient drop' is.**

AR: Simulations were considered converged when all residuals had fallen to a value of 1e-8 and the relative iteration-to-iteration change of the integrated drag was no greater than 1e-8.

*We have specified the tolerances used in section 3.2.2 (diff lines 250–253).*

---

**RC 7: Figures 2, 3, 5, 6, 8, 10 and 11 lack text within the legend. It was therefore difficult to confidently assess the validity of these results as well and the descriptions of the data contained within the results section and discussion. This was particularly pertinent to Figure 10 and the discussion in Section 4.3.**

AR: There was an issue with some fonts not being embedded within the figures of the initial upload. This was rectified during the discussion period and the pre-print file updated.

---

**RC 8: Discussion – The authors responsibly highlight that the results only relate two-dimensional structures. Some brief discussion should also be made that they are also relatively simple idealised structures as well.**

AR: We agree that some additional discussion on the idealized nature of the considered topographies is warranted. The simple topographies considered only serve as a starting point for additional studies and do not capture more complex features such as compound dune shapes and the complex interactions between potential separation, reattachment, and ensuing downstream effects.

*Add text to address the the simple nature of the profiles studied in section 5.3 (diff lines 549–551).*

## Response to Reviewer 2 (Orencio Duran Vinent) of

# Examination of Analytical Shear Stress Predictions for Coastal Dune Evolution

Orie Cecil, Nicholas Cohn, Matthew Farthing, Sourav Dutta, Andrew Trautz
*Earth Surface Dynamics,* egusphere-2024-855

---

**RC:** ***Reviewers' Comment***, AR: Authors' Response, *Manuscript Revisions*

---

**RC 1:** **As shown in Charru et al, Annu. Rev. Fluid Mech (2013) (Fig.3a), it is known that the linear approximation obtained by Jackson and Hunt (1975), and Hunt et al. (1988) (Eqs. 1-3 in the manuscript), overpredicts the value of the constant A (Eq. 5a) for $L/z_0 < 10^8$ compared to the full solution of the turbulent boundary layer in the limit of small amplitudes ($H/L << 1$). For the value $L/z_0 = 25000$ considered in the manuscript, the KSH model predicts A around 5, whereas the full solution would give A around 4. The authors should add this to their description of the KSH approximation and the discussion of model accuracy.**

AR: We would like to thank the reviewer for bringing this reference to our attention. Based on our analysis of the graphs, for $L/z_0 = 25000$, $kz_0 = \pi z_0/(2L) \approx 6.3\text{e}{-5}$ would correspond to $A$ around 5 as stated, while the full solution utilizing the damped Prandtl mixing length (Eq. 3 in the reference) returns a value around 3 in agreement with the value we report for $A$ in Eq. 19. On the same note, we predict the KSH value of $AB$ equivalent to $\mathcal{B}$ in the reference to be 1.45 while the figures indicate a value somewhat greater should be expected for a more complete calculation method in agreement with our SR result of $AB = 1.62$. This only strengthens the result and form of Eq. 19, notwithstanding the negligible term which we discuss more in our response to RC 6.

*This important context has been added to manuscript in section 4.2.2 (diff lines 389–396, 474–476).*

---

**RC 2:** **There is a mistake in Eqs.5b and 5c, in the actual approximation by Kroy et al. (2002), the term $2\ln(\pi/2)$ is neglected. This term comes from the term $2\ln(kL)$ in Eq.2, since for a periodic modulation of wavelength lambda we have $k = 2\pi/\lambda$, and by definition $L = \lambda/4$.**

AR: We thank the reviewer for pointing out this inconsistency between the text and equations of Kroy et al. (2002). We have clarified our use of the terms stemming from the logarithm of the base wave number in our presentation and discussion of Eq. 5.

*Clarification has been added to section 2.1 (diff lines 91–100).*

**RC 2.1:** **For clarity, in Eq.2 the term $\ln(k)$ should be replaced by $\ln(kL)$ since all lengths are rescaled by $L$ in this model.**

AR: Thank you for pointing out this oversight on our part. This correction has been implemented.

*Correction made in Eq. 2 (diff line 85).*

---

**RC 3: The value $L/z_0$ = 25000 used to evaluate the prediction from KSH seems arbitrary. If $L$ = 50 m and $z_0$ = 1e−3 m, as seems to be the case for the CFD, then $L/z_0$ = 50000. Furthermore, given the known overprediction of this approximation, the authors should add another prediction using $z_0$ = 1e−4 m, which is closer to the actual roughness of sand.**

AR: Thank you for pointing out this lack of clarity in the manuscript. The value of $L/z_0$ is indeed 25000 throughout as we have used $L$ = 25 m and $z_0$ = 1e−3 m. This has been stated clearly in the revised manuscript to avoid confusion.

*Clarification added in section 3.1 (diff line 218).*

As for the use of $z_0$ = 1e−3 m, we think this a reasonable value based on $z_0$ values used in other studies. For example, Walmsley and Howard (1985) used $z_0$ = 1e−3 m for their calculations and comparison to field data; Weng et al. (1991) fit field data with $z_0$ = 3e−3 m for sand in saltation; Araújo et al. (2013) used $z_0$ = 1e−4 m but reported that other values between 1e−5 m and 1e−3 m had a negligible effect on the shear stress in their simulations looking at separation; Jackson et al. (2020) used a value as high as $z_0$ = 5e−2 m in their simulations of unvegetated dunes in South Africa; Hesp and Smyth (2021) used $z_0$ = 5e−4 m in their study of flow over scarps; and similarly Bauer and Wakes (2022) used $z_0$ = 5e−4 m but considered $z_0$ = 5e−2 m noting that this resulted in larger values of wall shear stress. Altogether we believe that this points to $z_0$ = 1e−3 m as used in this study to be reasonable as it is well within the range of reported values used for simulations of unvegetated dunes. However, as indicated in RC1 and our response the results for the full boundary layer calculations presented in Charru et al, Annu. Rev. Fluid Mech (2013) (Fig.3a) do suggest a decrease in the error for prediction of $A$ between full calculations and asymptotic predictions as $L/z_0$ increases, while the error for $AB$ remains relatively constant. This observation has been noted and included in the discussion of the symbolic regression results to provide additional context to the reader.

*Additions made in section 4.2.2 (diff lines 394–396).*

---

**RC 4: There is a major confusion with the dune aspect ratio. In Fig.1, the aspect ratio H/L defines L as the dune's toe-crest length, whereas in all models L is defined as the half-length at half-height (the length between a point at half height and the crest, if I understood correctly). This means that there is no obvious way to compare the different simulated cases (H/L) with the relevant values in Fig.1. Here I have several suggestions:**

**RC 4.1: Please use different symbols for the different lengths, for example keeping L for the half-length at half-height but using L_base for the toe-crest length. You could also add a diagram illustrating the different terms to avoid confusion.**

AR: We would like to thank the reviewer for pointing out the lack of clarity between Fig. 1 and the remainder of the paper. We have used $L_{\text{base}}$ to refer to the toe-crest length throughout and added a diagram with the various important length scales. We agree that better distinguishing these two length scale terms with different symbols adds clarity for the reader, including demonstrating more clearly that the profiles investigated in this work do not generally exceed the angle of repose.

*Clarified the two length scales and their relation throughout and added a diagram of the relevant scales (now Figure 2).*

**RC 4.2: Given the toe-crest length is around twice the half-length at half-height, you could add another axis in Fig.1 to convert the standard aspect ratio plotted (using toe-crest length) to the new one used for the**

**simulations and all other figures. This is crucial because the simulated range in $H/L = [0.01, 0.5]$ only represents up to $H/L_{\text{base}} = 0.25$ in Fig.1, thus missing many relevant cases.**

AR: Due to the nature of the available data used to prepare Fig. 1, it would be difficult to accurately represent the distribution of $H/L$ of real dunes. This is in part because the ratio of $L$ to $L_{\text{base}}$ differs considerably depending on whether the profile is Gaussian, cosine, quartic, or bumped in shape. However, we have now included the relevant $L_{\text{base}}$ and $H/L_{\text{base}}$ values for the cosine and bump profiles to provide the context necessary to compare our results with Fig. 1. Additionally, Figure 13 now includes two axes, one with L and one with $L_{\text{base}}$ specifically applied to the Gaussian dune shape, to better connect the two length scales as it relates to implications for aeolian sediment transport predictions.

*Additions made to section 3.1 (diff lines 219–224) to clarify the relationship between our simulations and the possible range of coastal foredune aspect ratios. Additional axis for $H/L_{\text{base}}$ added to original Figure 13 (now 14).*

**RC 4.3: You should consider extending the simulated ratio $H/L$ (using half-length at half-height) all the way up to the avalanche angle ($H/L = 1.3$ and $H/L_{\text{base}} = 0.65$) to include the whole relevant range of foredunes' slopes. Also, please add the avalanche slope in Fig.1 for reference.**

AR: The range of $H/L$ values simulated captures $\sim$ 37.5% of coastal foredune data captured in Figure 1. Additionally, in RC8, the reviewer suggests that the comparison of predicted transport rate be limited to $H/L_{\text{base}} < 0.15$. We acknowledge that the present range of simulations does not cover all observed coastal foredune $H/L$ values and may be a limiting factor for our symbolic regression results on separated cases due to limited data for all profiles in the separated flow regime. However, we believe that the data presented is sufficient for an initial analysis and discussion of possible areas of improvement for linearized, asymptotic based models. Additionally, it would be expected as the low-slope assumptions for KSH continue to be exceeded for increasing $H/L$ (e.g., beyond the simulated limits) that deviations between KSH and the CFD-derived results will continue to increase. This reinforces the main findings that application of KSH to typical coastal foredunes, both vegetated and unvegetated, has limitations due to these slope criteria.

*Added some discussion suggesting that expanding the range of $H/L$ values is needed, particularly in addressing flow separation in the lee (see diff lines 431–435).*

---

**RC 5: There is a problem with using a Bump as a dune profile to compare to CFD. Because a Bump, as defined in Eq.6d, is not a smooth profile (there is a discontinuity in the slope and/or curvature at the base) it will experience flow separation at the lee-side and flow stagnation at the toe. Therefore, the predicted shear perturbation from KSH is not defined at the base ($\tau' < -1$) and has to be replaced by $\tau' = -1$, which means a vanishing bed shear stress ($\tau = 0$). Therefore, there is no meaning in using the values at these extreme locations to evaluate model accuracy (Fig.3e,f). Furthermore, the CFD predictions for the Bump (Fig.3c,d) don't really show the stagnation and flow separation expected at steep slopes, which suggests an issue with the simulations. The authors should either avoid the Bump case (and restrict only to smooth profiles) or properly discuss the complex physics involved.**

AR: It can be shown that the bump profile defined is in fact continuous and smooth. Following Nestruev 2020 (Smooth Manifolds and Observables, https://doi.org/10.1007/978-3-030-45650-4_2), pp. 13–14, start with the function

$$f(x) = \begin{cases} 0 & \text{for } y(x) \leq 0 \\ e^{-1/y(x)} & \text{for } y(x) > 0 \end{cases} \tag{1}$$

Upon substituting the polynomial $y(x) = 1 - b(x - \sigma)^2$ and multiplying by a leading coefficient $a$, one arrives at the Bump profile we have defined in the manuscript. Since $\sigma$ represents a simple shift and $a$ represents a constant scale factor, we take $\sigma = 0$ and $a = 1$ in the following to simplify the notation. Our function of interest is now

$$f(x) = \begin{cases} 0 & \text{for } 1 - bx^2 \leq 0 \\ e^{-(1-bx^2)^{-1}} & \text{for } 1 - bx^2 > 0 \end{cases} \tag{2}$$

It can be shown by induction that the $n$th derivative is of the form

$$f^{(n)}(x) = \begin{cases} 0 & \text{for } 1 - bx^2 \leq 0 \\ e^{-(1-bx^2)^{-1}} P_s(x) \ (1 - bx^2)^{-(n+1)} & \text{for } 1 - bx^2 > 0 \end{cases} \tag{3}$$

where $P_s(x)$ is a polynomial in $x$. Now, for the first derivative of Eq. (2), i.e., $n = 1$, we have

$$f^{(1)}(x) = \begin{cases} 0 & \text{for } 1 - bx^2 \leq 0 \\ e^{-(1-bx^2)^{-1}}(-2bx)(1 - bx^2)^{-2} & \text{for } 1 - bx^2 > 0 \end{cases} \tag{4}$$

which is of the form of Eq. (3). Furthermore, considering the $(n + 1)$th derivative yields

$$f^{(n+1)}(x) = \begin{cases} 0 & \text{for } 1 - bx^2 \leq 0 \\ e^{-(1-bx^2)^{-1}} \Big( -2bx\big(1 - bx^2\big)^n + P_s'(x)\big(1 - bx^2\big) & \\ \qquad +2bx(n+1)P_s(x) \Big) \big(1 - bx^2\big)^{-(n+2)} & \text{for } 1 - bx^2 > 0 \end{cases} \tag{5}$$

which again is of the form Eq. (3). Thus Eq. (2) is infinitely differentiable and $f^{(n)}(x) = 0 \ \forall \ x^2 > 1/b$. For $x^2 < 1/b$, $\lim_{x \to \pm\sqrt{1/b}} P_s(x)$ is some finite value for any $P_s(x)$, and therefore, by the product rule for limits, we need only show that $g(x) = \exp\Big(-\big(1 - bx^2\big)^{-1}\Big)(1 - bx^2)^{-(n+1)}$ vanishes as $x \to \pm\sqrt{1/b}$ for all $n$. By rearranging and applying L'Hospital's rule for $n = 1$ we have

$$\begin{aligned} \lim_{x \to \pm\sqrt{1/b}} \frac{\big(1 - bx^2\big)^{-2}}{\exp\Big(\big(1 - bx^2\big)^{-1}\Big)} &= \lim_{x \to \pm\sqrt{1/b}} \frac{2\big(1 - bx^2\big)^{-1}}{\exp\Big(\big(1 - bx^2\big)^{-1}\Big)} \\ &= \lim_{x \to \pm\sqrt{1/b}} \frac{-2}{\exp\Big(\big(1 - bx^2\big)^{-1}\Big)} \\ &= 0 \end{aligned} \tag{6}$$

And similarly for $n > 1$ with $n + 1$ applications of L'Hospital's rule. Therefore, the Bump profile is smooth being both infinitely differentiable and continuous.

We agree that the physics involved in predicting flow separation is complex and depends on a number of factors including dune form, windspeed, and other conditions as concluded in Walker and Nickling (2002). The separation bubble approach such as used by Kroy et al. (2002) and Schatz and Herrmann (2006) represent phenomenological fits of a cubic polynomial or ellipse, respectively, based solely on the dune geometry. However, Arùjo et al. (2013) shows that the length of the separating streamline as well as the reattachment angle is also dependent on the upwind shear velocity and concludes that an upwind shear velocity of $0.49\,\mathrm{m\,s^{-1}}$ is sufficient to initiate reverse transport in the dune lee. While extending the dune with a separating streamline

has enabled modeling the formation and integration of dunes of arbitrary topography, it is clear that some error is incurred in using such an approach to obtain approximations on the stoss slope and that potentially important phenomena are missed in the lee. Our CFD results predict separation on the bump profile for $H/L \geq 0.3$, the cosine profile for $H/L \geq 0.38$, and the cosine profile for $H/L \geq 0.5$; no separation is predicted for the Gaussian profile for the aspect ratios considered. However, our MSE results show no significant change in trend at the point when separation occurs and mirrors the trends for the Gaussian profile which never exhibits separation. Additionally, the KSH model predicts separation for much lower height-to-length ratios than the CFD or even the PySR Medium results which can be seen in Figures 4e and 7e in the revised manuscript. Limiting $\tau' \geq -1$ for the KSH results could result in a somewhat misleading error trend (not accounting for behavior over the stoss slope) where the error decreases as the CFD results approached separation while the modified KSH prediction remained stagnant before increasing again as the CFD results predict more negative values of $\tau'$ in growing the separation region.

As for flow over scarp like steep slopes at the dune toe, we would like to draw attention to the work of Hesp and Smyth (2021) and Bauer and Wakes (2022). Hesp and Smyth (2021) present CFD simulation results for flow over piecewise linear scarps with discontinuities in the slope at several angles finding no separation for angles less than or equal to 45° and that the upwind extent of flow separation varies with scarp height. Therefore, the presence of a discontinuity in slope does not guarantee the presence of separation at the dune toe. Additionally, Bauer and Wakes (2022) find in their simulations that the presence of scarps affects shear stress over the crest and in the lee as is to be expected in this low-speed flow regime. Thus, setting the calculated shear stress to zero in such areas without accounting for a modified effective dune shape such as is done for lee separation, ignores effects induced by the scarp over the rest of the dune surface. Additional simulations suggest that separation at the toe of the bump profile does not occur until around $H/L = 1$, while KSH predicts separation at the toe as low as $H/L = 0.2$ (see Figure 4c). This discrepancy in toe side separation is greatly improved by both SR results. Limiting $\tau'$ from the KSH model in this area as well could contribute to somewhat misleading results as discussed in the previous paragraph.

*We have included additional context on the practice of limiting the $\tau'$ prediction in predicted regions of separation in section 4.1 (diff lines 325–340).*

---

**RC 6: The symbolic regression result shown in Eq.19 is physically wrong, since a constant term in the relation between the Fourier transforms of the bed shear stress perturbation and the surface implies that the shear perturbation is proportional to the surface itself which doesn't make sense (the flow field is essentially scale-invariant in the limit of large $L/z_0$).**

AR: We would like to thank the reviewer for bringing this equation to our attention as there was a typographical error. The small constant term is actually a negligible real component of the $AB$ coefficient. We have confirmed that this was only a typographical error on our part and all results used the correct equation returned from PySR. That this small term is indeed negligible as illustrated in the figure below where solid lines represent the corrected expression, and the lighter dotted lines have neglected the small real component.

*Corrected Eq. 19 to read* $\mathcal{F}\left[\tau'\right] = \left(3.29|k| + \left(1.62i - 1.8\text{e}{-6}\right)k\right)\mathcal{F}\left[h\right]$ *(diff line 381–382).*

As for the physicality of the SR results in general, we have not explicitly enforced any physics principles or dimensional considerations in the SR approach beyond those which may be implicitly included by regressing on data generated by a physics based model, choosing to perform the regression in Fourier space, or by choosing an operator space which includes the operators of the linearized model. Eq. 19 represents the results of a generalized regression where both the expression and parameters are allowed to vary. The fact that this

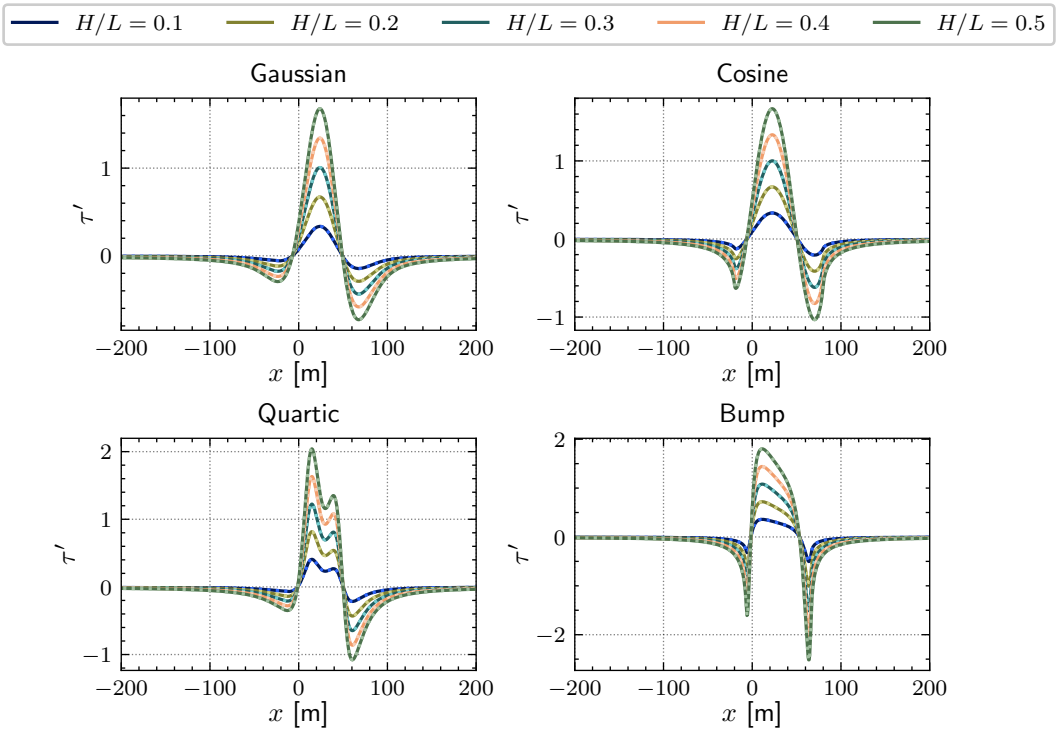


Figure 1: Shear stress perturbation predictions for all four profiles and several values of $H/L$. Solid dark lines represent the full SR expression. Lighter dotted lines represent the expression while neglecting the small real component of $AB$.

process returns an expression in agreement with the physics-based, linearized, asymptotic models not only emphasizes the applicability of the linearized models, but also the potential of SR to discover generalized expressions that capture the underlying physics strictly from data in some scenarios. While we have not explicitly enforced any physics principles in the present study, alternative methods of symbolic regression such as that proposed by Udrescu and Tegmark (2022) (https://doi.org/10.1126/sciadv.aay2631) do attempt to exploit typical simplifying properties that arise in physical systems. We believe that considering physics based constraints and simplifications would be a useful extension for improving the SR results, particularly when separated flow is present, in the future.

*We have clarified that process that led to Eq. 19 did not explicitly enforce any physics-based constraints (diff lines 383–387).*

**RC 6.1: There is a similar problem with Eq.20, which is quadratic on the wave number k. There are strong physical reasons behind the form of Eq.5a. If the authors want to improve the KSH model, the simplest way is to fit the parameters $A$ and $B$ to the CFD results on smooth profiles.**

AR: We agree that the form of Eq. 5a stands on a solid mathematical and physical basis in the linearized limit of small $H/L$ and corresponding slopes. However, there remains room for improvement and the limitations of the linearized result suggest that an improved model capable of capturing separation must take an alternate

or extended form that cannot be obtained from a simple fit of the linearized model parameters. In fact, by rearranging Eq. 20 one can arrive at

$$\mathcal{F}\left[\tau'\right] = \Big(4.84|k| + (3.26\text{e}{-6} + i2.20)k\Big)\mathcal{F}[h] + \Big((0.05 - i2.39\text{e}{-7}) - (7.56\text{e}{-6} + i5.1)|k|k - 11.23|k||k|\Big) \quad (7)$$

where the first grouping takes the same form as KSH and the second an extension involving the quadratic dependency on $k$ and a small constant term. We take care in the manuscript to point out that we do not take Eq. 20 as a particularly useful result, but merely the best result in terms of overall mse of the trials we conducted using symbolic regression (see diff lines 416–419, and 477–479). In fact, the results of Fig. 11 indicate that Eq. 20 is generally inferior to Eq. 19 with exception of the Quartic and Bump profiles for high $H/L$ where flow separation occurs.

*A minor topographical error in Eq. 20 was corrected in which the final term was missing an i (diff line 420).*

---

**RC 7: The way to measure the differences between the models, using MSE (Eq.18) is not particularly useful because it amplifies minor horizontal shifts in the simulations. For example, even a perfect prediction shifted horizontally by 1m would lead to a large MSE. You should also include the difference in the maximum (and minimum) shear stress perturbations between the models.**

AR: We believe that this concern is minor for the present study as the KSH and SR predictions were made directly on the profiles extracted from the CFD discretization. However, we have included tabulations of the differences between the local minimums upstream and downstream of the dune crests as well as the maximum predicted shear stress perturbation and expanded our discussions to include these additional data points.

*Added tables 2-4 containing the differences in extrema prediction as well as expanded the results sections to discuss this additional data (see diff lines 353–362, 407–415, and 428–435).*

---

**RC 8: The examples in Fig.12 for the predicted transport rate seem completely arbitrary. The linear models have been successfully used to simulate unvegetated dunes in many different situations mainly because the aspect ratio of dunes (using toe-crest length) is always less than ≈ 0.15. Steeper dunes have to be vegetated, but then there is essentially no sand transport. The authors should either use actual dunes shapes or at least the aspect ratios of actual mobile (unvegetated) dunes to compare sand transport rates.**

AR: The cases presented in Figure 12 are meant to be representative of the broader set of simulations to demonstrate general differences between the PySR and Kroy model results both in terms of direct differences in spatial bed shear stress patterns and implications for sediment transport. Although the original suite of results shown in Figure 12 did not exceed any angle of repose, as per the reviewer's suggestion we have focused on representative cases with lower slopes. Now the steepest case in this series of plots is a gaussian profile with H = 6 m and L = 25 m which represents a $H/L$ ratio of 0.24 and a $H/L_{\text{base}}$ of less than 0.1. These cases all therefore reflect dune topographies that could represent bare sand, unvegetated dunes.

*Changed cases presented in Figure 12 (now 13) and relevant discussion (diff line 511).*

**RC 8.1: The transport equation (Eq.21) is wrong for aeolian sand transport. Please use the one in Martin and Kok, Science Advances (2017), which is consistent with several wind tunnel measurements and transport simulations.**

AR: There are numerous equations that represent theoretical aeolian sediment transport rates under ideal conditions. The majority of these equations, such as that presented by Bagnold, are based on a third order scaling of the shear velocity. Although, indeed, there is debate over the whether linear flux scaling with shear stress is more appropriate (Martin and Kok, 2017), and there remains some uncertainty whether indeed the saltation height is shear invariant (see Cohn, N., Dickhudt, P., & Brodie, K. 2022. Remote observations of aeolian saltation. Geophysical Research Letters) which limits the potential universality of using this proposed formulation.

Regardless, for the purposes of this manuscript, the aeolian sediment transport calculations are supplemental to primarily inform implications of the differences in wind flow dynamics between PySR/OpenFoam outputs and those of KSH. Thus, we agree that different formulations - of which there are many reflecting uncertainty in the ability to accurately model aeolian transport using shear properties alone - would result in different magnitudes represented in Figure 13 arising out of the use of Eq 21. However, the trends in that there are larger deviations in $q$ with increasing $H/L$ ratios and/or increasing $\tau$ would not change. Thus, since we utilize an existing numerical model that does not currently include the Martin and Kok (2017) formulation in it, we do not explicitly include reference to this formulation in the text or in any calculations. However, we have added a line to the text to explicitly note that other formulations exist in the literature that do have different flux scaling relationships.

*Added context for alternative sediment flux calculations in section 5.2 (diff lines 496–497).*

**RC 8.2: The data in Fig.12f seems inconsistent with Fig.3b. In Fig.3b, both CFD and KSH are quite similar for $H/L = 0.4$, but they are quite different in Fig.12f for $H/L = 0.5$.**

AR: The results in the second row of Figure 12 (now 13) present the actual shear stress prediction using an upstream value of $\tau_0 = 0.6$ while Fig. 3 (now 4) presents the shear stress perturbation $\tau'$. Additionally, in response to RC8 the case for $H/L = 0.5$ has been replaced such that the highest $H/L$ ratio is 0.24.

---

**RC 9: In lines 100-105. It is not true that the KSH model cannot be applied to scarps. In fact, a better version of this model (given by Weng et al. 1991) is already implemented in the Coastal Dune Model which certainly simulates dune recovery after erosion and scarp formation (Duran and Moore, Nature Clim. Change, 2015). In this case, similarly as for the Bump, the shear stress perturbation reaches $< -1$, and the only physically meaningful condition is $\tau = 0$ (which follows from flow stagnation).**

AR: We would refer back to our response to RC5, where we discuss the various issues with applying either phenomenological fits for separating streamlines or simply setting the shear stress to zero.

*We have changed the language to more accurately address the issues with applying KSH type models to dunes with locally steep features such as scarps (diff lines 103–113).*

---

**RC 10: In addition to the technical issues mentioned above, I see two important conceptual problems. The manuscript introduces the main limitation of the linear models (e.g. KSH) using the steep slopes of the foredunes or vegetated dunes at the beach. However, they never compare the models using an actual foredune profile. Furthermore, the relative difference of the maximum shear stress perturbation between the KSH and the CFD for a gaussian hill seems to improve for larger $H/L$ (Fig.3a,b) instead of getting worse, which would undercut the main purpose of the manuscript. There is also a consistency issue here because steep foredunes (where model's predictions would be worst) are covered by vegetation (that is why they can be so steep in the first place) and therefore there is no active sand transport on**

**the crest and lee side. On the other hand, active dunes would have milder slopes and thus the model would be more suitable. These things should be properly discussed to help the reader understand the scope and meaning of the actual problems with flow simulations.**

AR: Our results do indicate that the maximum shear stress prediction error between KSH and CFD improve for increasing $H/L$ above $H/L \approx 0.26$. However, the overall MSE continues to increase for all profiles indicating differences at the minima as well as in the overall distribution. Moreover, this is not true in general as can be seen with the bump profile which exhibits consistent growth of all error measures with increasing $H/L$.

*These nuances have been discussed in the revised version with the addition of the tabulated values of extrema error in response to RC7.*

We agree that vegetation adds additional complexity to the system both by stabilizing steep dunes and also by limiting sediment transport. However, in many models the effects of vegetation are implemented as a correction factor to the topographically driven shear stress, and so the accuracy of the shear perturbation prediction over the steep unvegetated surface is still a fundamental concern. We have included some additional discussion of these considerations to the revised manuscript.

*Added discussion of vegetation considerations in section 5.3 (diff lines 539–543).*

---

**RC 11: The second conceptual problem is related to the general assumption behind the manuscript, that somehow there should be a simple shortcut to improve the calculation of the bed shear stress under arbitrary topographic conditions. These models (in particular the 3D version in Weng et al. 1991) are already very powerful since they allowed for the first time physical simulations of 3D dune formation and interactions, formation of dune fields (Duran et al., ESPL, 2010), the formation of parabolic dunes (Duran and Herrmann, PRL, 2006), coastal dunes, dunes on Mars (Parteli and Herrmann, PRL, 2007), etc. This implementation of the Weng et al. (1991) approximation is very fast to compute and works (with the proper extension for the flow-separation region) for arbitrary topographies. Of course, it is not perfect and it is important to evaluate its accuracy, but it should be clearly stated that it represents a actual physical approximation, not a phenomenological fitting, and cannot be easily replaced by a data-based approach that requires many 3D CFD simulations to provide data. I would suggest to focus on using CFD to improve the parameters in KSH as a way to move forward in the field without having to start from scratch with data-based approaches after +40 years of physical insight and meaningful applications.**

AR: We agree that there is a lot of value in the existing approaches to modeling wind flow dynamics using KSH, as has been demonstrated by the broad literature on this topic applied to a range of complex 1D and 2D landforms (e.g., see lines 40–45, 114–116, and 474–476 of the revised manuscript). Perhaps inspired by the capabilities for numerical models leveraging KSH to replicate these dynamics, this has also spurred such models to be pushed to the limit to replicate the exact dynamics of real world systems. KSH and all models will have limitations in application to real world systems where the specific local details of topography and vegetation matter. The engineering and scientific need on this topic therefore triggers either (1) adapting existing approaches and/or (2) testing new approaches. In this application we already note the ability to do both of these. Specifically, in the discussion section we discuss how these outputs could inform better KSH coefficient fits, perhaps allowing for an extension of KSH to a broader range of $H/L$ conditions. This could provide considerable value in rapid estimation of 1D and 2D shear stress in real world landforms.

However, independent of altering equation coefficients, there will remain limitations of the KSH approach

to real world topographies given the simplicity of the approach. CFD model simulations, while very computationally demanding, inherently represent the non-linearities of the system that may be important for representing shear and sediment transport. However, CFD model results are generally impractical to run over dynamically changing topography. The symbolic regression approaches we present here are a step towards leveraging CFD model outputs without the real-time computational costs of CFD. We recognize there are challenges associated with using data driven methodologies namely the burden of generating data using 3D CFD simulations and have acknowledged these in section 5.3.

*We've added and/or edited language to better emphasize that KSH type models represent physical approximations to the Navier-Stokes equations and their utility (diff lines 78–80, and 116–119).*